

# Spin dephasing in *n*-typed GaAs quantum wells

M. Q. Weng and M. W. Wu\*

Structure Research Laboratory, University of Science & Technology of China, Academia Sinica, Hefei, Anhui, 230026, China  
 Department of Physics, University of Science & Technology of China, Hefei, Anhui, 230026, China<sup>†</sup>

(Dated: March 9, 2021)

We perform a many-body study of the spin dephasing due to the D'yakonov-Perel' effect in *n*-typed GaAs (100) quantum wells for high temperatures ( $\geq 120$  K) under moderate magnetic fields in the Voigt configuration by constructing and numerically solving the kinetic Bloch equations. We include all the spin conserving scattering such as the electron-phonon, the electron-nonmagnetic impurity as well as the electron-electron Coulomb scattering in our theory and investigate how the spin dephasing rate is affected by the initial spin polarization, temperature, impurity, magnetic field as well as the electron density. The dephasing obtained from our theory contains not only that due to the effective spin-flip scattering first proposed by D'yakonov and Perel' [Zh. Eksp. Teor. Fiz. **60**, 1954(1971)[Sov. Phys.-JETP **38**, 1053(1971)]], but also the recently proposed many-body dephasing due to the inhomogeneous broadening provided by the DP term [Wu, J. Supercond.:Incorp. Novel Mechanism **14**, 245 (2001); Wu and Ning, Eur. Phys. J. B **18**, 373 (2000)]. We show that for the electron densities we study, the spin dephasing rate is dominated by the many-body effect. Equally remarkable is that we are now able to investigate the spin dephasing with extra large spin polarization (up to 100 %) which has not been discussed both theoretically and experimentally. We find a dramatic decrease of the spin dephasing rate for large spin polarizations. The spin dephasing time (SDT), which is defined as the inverse of the spin dephasing rate, we get at low initial spin polarization is in agreement with the experiment both qualitatively and quantitatively.

PACS numbers: PACS: 71.10.-w, 67.57.Lm, 72.25.Rb, 73.61.Ey

## I. INTRODUCTION

The resent development of ultrafast nonlinear optical experiments<sup>1,2,3,4,5,6,7,8,9,10,11,12,13,14</sup> has stimulated immense interest in spintronics in semiconductors as it shows great potential of using the spin degree of freedom of electrons in place of/in addition to the charge degree of freedom for device application such as qubits, quantum memory devices, and spin transistors.

In order to make use of the spin degree of freedom in semiconductor spintronics, it is crucial to have a thorough understanding of spin dephasing mechanism. Three spin dephasing mechanisms have been proposed in semiconductors:<sup>15,16</sup> the Elliot-Yafet (EY) mechanism,<sup>17,18</sup> the D'yakonov-Perel' (DP) mechanism,<sup>19</sup> and the Bir-Aronov-Pikus (BAP) mechanism.<sup>20</sup> In the EY mechanism, the spin-orbit interaction leads to mixing of wave functions of opposite spins. This mixing results in a nonzero electron spin flip due to impurity and phonon scattering. The DP mechanism is due to the spin-orbit interaction in crystals without inversion center, which results in spin state splitting of the conduction band at  $k \neq 0$ . This is equivalent to an effective magnetic field acting on the spin, with its magnitude and orientation depending on  $\mathbf{k}$ . Finally, the BAP mechanism is originated from the mixing of heavy hole and light hole bands induces by spin-orbit coupling. Spin-flip (SF) scattering of electrons by holes due to the Coulomb interaction is therefore permitted, which gives rise to spin dephasing. The dephasing rates of these mechanisms for low polarized system are calculated in the framework of single particle approximation.<sup>15</sup> For GaAs, the EY mech-

anism is less effective under most conditions, due to the large band gap and low scattering rate for high quality samples. The BAP mechanism is important for either *p*-doped or insulating GaAs. For *n*-doped samples, however, as holes are rapidly recombined with electrons due to the presence of a large number of electrons, spin dephasing due to the regular BAP mechanism is blocked. Therefore, the DP mechanism (or possibly the EY mechanism under certain conditions) is the main mechanism of spin dephasing for *n*-type GaAs.

It is important to note that all the mechanisms above either provide or are treated as SF scattering. Spin-conserving (SC) scattering, such as the ordinary Coulomb scattering, electron-phonon and electron-nonmagnetic impurity scattering which has been extensively studied in connection with optical dephasing and relaxation,<sup>21</sup> are commonly believed to be unable to cause spin dephasing as the corresponding interaction Hamiltonians commute with the total spin operator.

Recently Wu proposed a many-body kinetic theory<sup>22</sup> to study the spin precession and spin dephasing in insulating ZnSe/Zn<sub>1-x</sub>Cd<sub>x</sub>Se quantum well (QW),<sup>23</sup> *n*-typed bulk GaAs samples,<sup>24</sup> and *n*-typed GaAs (110) QW,<sup>25</sup> under moderate magnetic fields in the Voigt configuration. Based on this many-body theory, he further showed that the SC scattering can also cause spin dephasing in the presence of inhomogeneous broadening.<sup>22,24,25,26,27</sup> This novel spin dephasing mechanism has long been overlooked in the literature. Differing from the earlier study of the spin dephasing which comes from SF scattering, the spin dephasing through inhomogeneous broadening is caused by irreversibly disrupting the phases between

spin dipoles and is therefore a many-body effect.<sup>22,26,27</sup> Very recently we have shown that this inhomogeneous broadening effect also plays an important role in the spin transport<sup>28,29</sup>.

In this paper, we study the spin dephasing in  $n$ -doped GaAs (100) QW's. We calculate the SDT by numerically solving the many-body kinetic equations with all the scattering included. Differing from the previous investigation in the bulk case where we are only able to get the SDT qualitatively,<sup>24</sup> here we get the SDT quantitatively thanks to the reduction of dimension in the momentum space. Moreover as we include the electron-electron Coulomb scattering in our calculation, for the first time we are able to study the spin dephasing with extra large initial spin polarization (up to 100 %) which has not been investigate both experimentally and theoretically.

We organize the paper as follows: We present our model and the kinetic equations in Sec. II. Then in Sec. III(A) we show the time evolution of the spin signal where we show the contribution of the Coulomb scattering to the spin dephasing. In Sec. III(B) we investigate how the SDT changes with the variation of the initial spin polarization. The temperature dependence of the SDT under different spin polarization is discussed in detail in Sec. III(C), where we also highlight the difference between the present many-body theory and the earlier simplified theory. In Sec. III(D) we show the magnetic field dependence of the SDT. Finally we discuss how the electron density affect the SDT. We present the conclusion and summary in Sec. IV.

## II. KINETIC EQUATIONS

We start our investigation from an  $n$ -doped (100) GaAs QW with well width  $a$ . The growth direction is assumed to be  $z$ -axis. A moderate magnetic field  $\mathbf{B}$  is applied along the  $x$  axis. Due to the confinement of the QW, the momentum states along  $z$  axis are quantized. Therefore the electron states are characterized by a subband index  $n$  and a two dimensional wave vector  $\mathbf{k} = (k_x, k_y)$  together with a spin index  $\sigma$ . In the present paper, the subband separation is assumed to be large enough so that only the lowest subband is populated and the transition to the upper subbands is unimportant. Therefore, one only needs to consider the lowest subband. For  $n$ -doped samples, spin dephasing mainly comes from the DP mechanism.<sup>19</sup> With the DP term included, the Hamiltonian of the electrons in the QW takes the form:

$$H = \sum_{\mathbf{k}\sigma\sigma'} \left\{ \varepsilon_{\mathbf{k}} + [g\mu_B \mathbf{B} + \mathbf{h}(\mathbf{k})] \cdot \frac{\vec{\sigma}_{\sigma\sigma'}}{2} \right\} c_{\mathbf{k}\sigma}^\dagger c_{\mathbf{k}\sigma'} + H_I. \quad (1)$$

Here  $\varepsilon_{\mathbf{k}} = \mathbf{k}^2/2m^*$  is the energy of electron with wavevector  $\mathbf{k}$  and effective mass  $m^*$ .  $\vec{\sigma}$  are the Pauli matrices. In QW system, the DP term is composed of the Dresselhaus term<sup>30</sup> and the Rashba term.<sup>31,32</sup> The Dresselhaus term is due to the lack of inversion symmetry in the zinc-blende crystal Brillouin zone and is sometimes referred to as bulk inversion asymmetry (BIA) term. For the (100) GaAs QW system, it can be written as<sup>33,34</sup>

$$\begin{aligned} h_x^{\text{BIA}}(\mathbf{k}) &= \gamma k_x (k_y^2 - \langle k_z^2 \rangle), \\ h_y^{\text{BIA}}(\mathbf{k}) &= \gamma k_y (\langle k_z^2 \rangle - k_x^2), \\ h_z^{\text{BIA}}(\mathbf{k}) &= 0. \end{aligned} \quad (2)$$

Here  $\langle k_z^2 \rangle$  represents the average of the operator  $-(\frac{\partial}{\partial z})^2$  over the electronic state of the lowest subband and is therefore  $(\pi/a)^2$ .  $\gamma = (4/3)(m^*/m_{cv})(1/\sqrt{2m^*E_g})(\eta/\sqrt{1-\eta/3})$  and  $\eta = \Delta/(E_g + \Delta)$ , in which  $E_g$  denotes the band gap;  $\Delta$  represents the spin-orbit splitting of the valence band;  $m^*$  standing for the electron mass in GaAs; and  $m_{cv}$  is a constant close in magnitude to free electron mass  $m_0$ .<sup>16</sup> Whereas the Rashba term appears if the self-consistent potential within a QW is asymmetric along the growth direction and is therefore referred to as structure inversion asymmetry (SIA) contribution. Its scale is proportional to the interface electric field along the growth direction. For narrow band-gap semiconductors such as InAs, the Rashba term is the main spin-dephasing mechanism; whereas in the wide band-gap semiconductors such as GaAs, the Dresselhaus term is dominant. In the present paper, we will take only the Dresselhaus term into consideration as we focus on the spin dephasing in GaAs QW. The interaction Hamiltonian  $H_I$  is composed of Coulomb interaction  $H_{ee}$ , electron-phonon interaction  $H_{ph}$ , as well as electron-impurity scattering  $H_i$ . Their expressions can be found in textbooks.<sup>21,35</sup>

We construct the kinetic Bloch equations by the nonequilibrium Green function method<sup>21</sup> as follows:

$$\dot{\rho}_{\mathbf{k},\sigma\sigma'} = \dot{\rho}_{\mathbf{k},\sigma\sigma'}|_{\text{coh}} + \dot{\rho}_{\mathbf{k},\sigma\sigma'}|_{\text{scatt}} \quad (3)$$

Here  $\rho_{\mathbf{k}}$  represents the single particle density matrix. The diagonal elements describe the electron distribution functions  $\rho_{\mathbf{k},\sigma\sigma} = f_{\mathbf{k}\sigma}$ . The off-diagonal elements  $\rho_{\mathbf{k},\frac{1}{2}-\frac{1}{2}} \equiv \rho_{\mathbf{k}}$  describe the inter-spin-band polarizations (coherence) of the spin coherence.<sup>23</sup> Note that  $\rho_{\mathbf{k},-\frac{1}{2}\frac{1}{2}} \equiv \rho_{\mathbf{k},\frac{1}{2}-\frac{1}{2}}^* = \rho_{\mathbf{k}}^*$ . Therefore,  $f_{\mathbf{k}\pm\frac{1}{2}}$  and  $\rho_{\mathbf{k}}$  are the quantities to be determined from Bloch equations.

The coherent part of the equation of motion for the electron distribution function is given by

$$\frac{\partial f_{\mathbf{k},\sigma}}{\partial t}|_{\text{coh}} = -2\sigma\{[g\mu_B B + h_x(\mathbf{k})]\text{Im}\rho_{\mathbf{k}} + h_y(\mathbf{k})\text{Re}\rho_{\mathbf{k}}\} + 4\sigma\text{Im}\sum_{\mathbf{q}}V_{\mathbf{q}}\rho_{\mathbf{k}+\mathbf{q}}^*\rho_{\mathbf{k}}, \quad (4)$$

where  $V_{\mathbf{q}} = 4\pi e^2/[\kappa_0(q + q_0)]$  is the 2D Coulomb matrix element under static screening.  $q_0 = (e^2 m^*/\kappa_0) \sum_{\sigma} f_{\mathbf{k}=0,\sigma}$  and  $\kappa_0$  is the static dielectric constant. The first term on the right hand side (RHS) of Eq. (4) describes spin precession of electrons under the magnetic field  $\mathbf{B}$  as well as the effective magnetic field  $\mathbf{h}(\mathbf{k})$  due to the DP effect. The scattering terms of electron distribution functions in the Markovian limit are given by

$$\begin{aligned} \frac{\partial f_{\mathbf{k},\sigma}}{\partial t}|_{\text{scatt}} = & \left\{ -2\pi \sum_{\mathbf{q}q_z\lambda} g_{\mathbf{Q}\lambda}^2 \delta(\varepsilon_{\mathbf{k}} - \varepsilon_{\mathbf{k}-\mathbf{q}} - \Omega_{\mathbf{q}q_z\lambda}) [N_{\mathbf{q}q_z\lambda}(f_{\mathbf{k}\sigma} - f_{\mathbf{k}-\mathbf{q}\sigma}) + f_{\mathbf{k}\sigma}(1 - f_{\mathbf{k}-\mathbf{q}\sigma}) - \text{Re}(\rho_{\mathbf{k}}\rho_{\mathbf{k}-\mathbf{q}}^*)] \right. \\ & - 2\pi N_i \sum_{\mathbf{q}} U_{\mathbf{q}}^2 \delta(\varepsilon_{\mathbf{k}} - \varepsilon_{\mathbf{k}-\mathbf{q}}) [f_{\mathbf{k}\sigma}(1 - f_{\mathbf{k}-\mathbf{q}\sigma}) - \text{Re}(\rho_{\mathbf{k}}\rho_{\mathbf{k}-\mathbf{q}}^*)] - 2\pi \sum_{\mathbf{q}\mathbf{k}'\sigma'} V_{\mathbf{q}}^2 \delta(\varepsilon_{\mathbf{k}-\mathbf{q}} - \varepsilon_{\mathbf{k}} + \varepsilon_{\mathbf{k}'} - \varepsilon_{\mathbf{k}'-\mathbf{q}}) \\ & \left. \left[ (1 - f_{\mathbf{k}-\mathbf{q}\sigma})f_{\mathbf{k}\sigma}(1 - f_{\mathbf{k}'\sigma'})f_{\mathbf{k}'-\mathbf{q}\sigma'} + \frac{1}{2}\rho_{\mathbf{k}}\rho_{\mathbf{k}-\mathbf{q}}^*(f_{\mathbf{k}'\sigma'} - f_{\mathbf{k}'-\mathbf{q}\sigma'}) + \frac{1}{2}\rho_{\mathbf{k}'}\rho_{\mathbf{k}'-\mathbf{q}}^*(f_{\mathbf{k}-\mathbf{q}\sigma} - f_{\mathbf{k}\sigma}) \right] \right\} \\ & - \{\mathbf{k} \leftrightarrow \mathbf{k} - \mathbf{q}, \mathbf{k}' \leftrightarrow \mathbf{k}' - \mathbf{q}\}, \end{aligned} \quad (5)$$

in which  $\{\mathbf{k} \leftrightarrow \mathbf{k} - \mathbf{q}, \mathbf{k}' \leftrightarrow \mathbf{k}' - \mathbf{q}\}$  stands for the same terms as in the previous  $\{\}$  but with the interchange  $\mathbf{k} \leftrightarrow \mathbf{k} - \mathbf{q}$  and  $\mathbf{k}' \leftrightarrow \mathbf{k}' - \mathbf{q}$ . The first term inside the braces on the RHS of Eq. (5) comes from the electron-phonon interaction.  $\lambda$  stands for the different phonon modes, *i.e.*, one longitude optical (LO) phonon mode, one longitudinal acoustic (AC) phonon mode due to the deformation potential, and two AC modes due to the transverse piezoelectric field.  $g_{\mathbf{q}q_z\lambda}$  are the matrix elements of electron-phonon coupling for mode  $\lambda$ . For LO phonons,  $g_{\mathbf{q}q_z\text{LO}}^2 = \{4\pi\alpha\Omega_{\text{LO}}^{3/2}/[\sqrt{2\mu}(q^2 + q_z^2)]\}|I(iq_z)|^2$  with  $\alpha = e^2\sqrt{\mu/(2\Omega_{\text{LO}})}(\kappa_{\infty}^{-1} - \kappa_0^{-1})$ .  $\kappa_{\infty}$  is the optical dielectric constant and  $\Omega_{\text{LO}}$  is the LO phonon frequency. The form

factor  $|I(iq_z)|^2 = \pi^2 \sin^2 y/[y^2(y^2 - \pi^2)^2]$  with  $y = q_z a/2$ .  $N_{\mathbf{q}q_z\lambda} = 1/[\exp(\Omega_{\mathbf{q}q_z\lambda}/k_B T) - 1]$  is the Bose distribution of phonon mode  $\lambda$  at temperature  $T$ . The second term inside the braces on the RHS of Eq. (5) results from the electron-impurity scattering under the random phase approximation with  $N_i$  denoting the impurity concentration.  $U_{\mathbf{q}}^2 = \sum_{q_z} \{4\pi Z_i e^2/[\kappa_0(q^2 + q_z^2)]\}^2 |I(iq_z)|^2$  is the electron-impurity interaction matrix element with  $Z_i$  stands for the charge number of the impurity.  $Z_i$  is assumed to be 1 throughout our calculation. The third term is the contribution of the Coulomb interaction. Similarly, the coherent and the scattering parts of the spin coherence are given by

$$\frac{\partial \rho_{\mathbf{k}}}{\partial t}|_{\text{coh}} = \frac{1}{2}[ig\mu_B B + ih_x(\mathbf{k}) + h_y(\mathbf{k})](f_{\mathbf{k}\frac{1}{2}} - f_{\mathbf{k}-\frac{1}{2}}) + i \sum_{\mathbf{q}} V_{\mathbf{q}} [(f_{\mathbf{k}+\mathbf{q}\frac{1}{2}} - f_{\mathbf{k}+\mathbf{q}-\frac{1}{2}})\rho_{\mathbf{k}} - \rho_{\mathbf{k}+\mathbf{q}}(f_{\mathbf{k}\frac{1}{2}} - f_{\mathbf{k}-\frac{1}{2}})], \quad (6)$$

$$\begin{aligned} \frac{\partial \rho_{\mathbf{k}}}{\partial t}|_{\text{scatt}} = & \left\{ \pi \sum_{\mathbf{q}q_z\lambda} g_{\mathbf{Q}\lambda}^2 \delta(\varepsilon_{\mathbf{k}} - \varepsilon_{\mathbf{k}-\mathbf{q}} - \Omega_{\mathbf{q}q_z\lambda}) [\rho_{\mathbf{k}-\mathbf{q}}(f_{\mathbf{k}\frac{1}{2}} + f_{\mathbf{k}-\frac{1}{2}}) + (f_{\mathbf{k}-\mathbf{q}\frac{1}{2}} + f_{\mathbf{k}-\mathbf{q}-\frac{1}{2}} - 2)\rho_{\mathbf{k}} - 2N_{\mathbf{q}q_z\lambda}(\rho_{\mathbf{k}} - \rho_{\mathbf{k}-\mathbf{q}})] \right. \\ & + \pi N_i \sum_{\mathbf{q}} U_{\mathbf{q}}^2 \delta(\varepsilon_{\mathbf{k}} - \varepsilon_{\mathbf{k}-\mathbf{q}}) [(f_{\mathbf{k}\frac{1}{2}} + f_{\mathbf{k}-\frac{1}{2}})\rho_{\mathbf{k}-\mathbf{q}} - (2 - f_{\mathbf{k}-\mathbf{q}\frac{1}{2}} - f_{\mathbf{k}-\mathbf{q}-\frac{1}{2}})\rho_{\mathbf{k}}] \\ & - \sum_{\mathbf{q}\mathbf{k}'} \pi V_{\mathbf{q}}^2 \delta(\varepsilon_{\mathbf{k}-\mathbf{q}} - \varepsilon_{\mathbf{k}} + \varepsilon_{\mathbf{k}'} - \varepsilon_{\mathbf{k}'-\mathbf{q}}) \left( (f_{\mathbf{k}-\mathbf{q}\frac{1}{2}}\rho_{\mathbf{k}} + \rho_{\mathbf{k}-\mathbf{q}}f_{\mathbf{k}-\frac{1}{2}})(f_{\mathbf{k}'\frac{1}{2}} - f_{\mathbf{k}'-\mathbf{q}\frac{1}{2}} + f_{\mathbf{k}'-\frac{1}{2}} - f_{\mathbf{k}'-\mathbf{q}-\frac{1}{2}}) \right. \\ & + \rho_{\mathbf{k}} [(1 - f_{\mathbf{k}'\frac{1}{2}})f_{\mathbf{k}-\mathbf{q}\frac{1}{2}} + (1 - f_{\mathbf{k}'-\frac{1}{2}})f_{\mathbf{k}-\mathbf{q}-\frac{1}{2}} - 2\text{Re}(\rho_{\mathbf{k}'}^*\rho_{\mathbf{k}-\mathbf{q}})] - \rho_{\mathbf{k}-\mathbf{q}}[f_{\mathbf{k}'\frac{1}{2}}(1 - f_{\mathbf{k}'-\mathbf{q}\frac{1}{2}}) \\ & \left. \left. + (1 - f_{\mathbf{k}'-\frac{1}{2}})f_{\mathbf{k}'-\mathbf{q}-\frac{1}{2}} - 2\text{Re}(\rho_{\mathbf{k}'}^*\rho_{\mathbf{k}'-\mathbf{q}})\right) \right\} - \{\mathbf{k} \leftrightarrow \mathbf{k} - \mathbf{q}, \mathbf{k}' \leftrightarrow \mathbf{k}' - \mathbf{q}\}. \end{aligned} \quad (7)$$

The initial conditions are taken at  $t = 0$  as:

$$\rho_{\mathbf{k}}|_{t=0} = 0 \quad (8)$$

$$f_{\mathbf{k}\sigma}|_{t=0} = 1/\{\exp[(\varepsilon_{\mathbf{k}} - \mu_{\sigma})/k_B T] + 1\} \quad (9)$$

where  $\mu_\sigma$  is the chemical potential for spin  $\sigma$ . The condition  $\mu_{\frac{1}{2}} \neq \mu_{-\frac{1}{2}}$  gives rise to the imbalance of the electron densities of the two spin bands. Eqs. (3) through (7) together with the initial conditions Eqs. (8) and (9) comprise the complete set of kinetic Bloch equations of our investigation.

### III. NUMERICAL RESULTS

The kinetic Bloch equations form a set of nonlinear equations. All the unknowns to be solved appear in the scattering terms. Specifically, the electron distribution function is no longer a Fermi distribution because of the existence of the anisotropic DP term  $\mathbf{h}(\mathbf{k})$ . This term in the coherent part drives the electron distribution away from an isotropic Fermi distribution. The scattering term attempts to randomize electrons in  $\mathbf{k}$ -space. Obviously, both the coherent part and the scattering terms have to be solved self-consistently to obtain the distribution function and the spin coherence.

$\kappa_\infty$	10.8	$\kappa_0$	12.9
$\omega_0$	35.4 meV	$m^*$	0.067 $m_0$
$\Delta$	0.341 eV	$E_g$	1.55 eV
$g$	0.44		

TABLE I: Parameters used in the numerical calculations

We numerically solve the kinetic Bloch equations in such a self-consistent fashion to study the spin precession between the spin-up and -down bands. We include electron-phonon scattering and the electron-electron interaction throughout our computation. As we concentrate on the relatively high temperature regime ( $T \geq 120$  K) in the present study, for electron-phonon scattering we only need to include electron-LO phonon scattering. Electron-impurity scattering is sometimes excluded. As discussed in the previous paper,<sup>23,36</sup> irreversible spin dephasing can be well defined by the slope of the envelope of the incoherently summed spin coherence  $\rho(t) = \sum_{\mathbf{k}} |\rho_{\mathbf{k}}|$ . The material parameters of GaAs for our calculation are tabulated in Table I.<sup>37</sup> The method of the numerical calculation has been laid out in detail in our previous paper on the DP mechanism in 3D systems.<sup>24</sup> The difference is that here we are able to get the results quantitatively instead of only qualitatively as in our previous 3D case, thanks to the smaller dimension in the momentum space. Our main results are plotted in Figs. 1 to 10. In these calculations the total electron density  $N_e$  and the applied magnetic field  $B$  are chosen to be  $4 \times 10^{11} \text{ cm}^{-2}$  and 4 T respectively unless otherwise specified. The width of the quantum well is chosen typical to be 15 nm except in the last two figures.

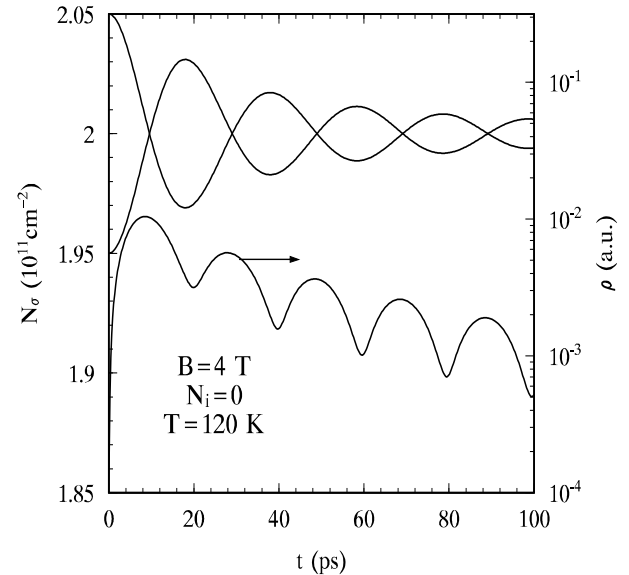


FIG. 1: Electron densities of up spin and down spin and the incoherently summed spin coherence  $\rho$  versus time  $t$  without taking account the Coulomb scattering for a GaAs QW with initial spin polarization  $P = 2.5\%$ , at  $T = 120$  K. Note the scale of the spin coherence is on the right side of the figure.

#### A. Temporal evolution of the spin signal

We first study the temporal evolution of the spin signal in a GaAs QW at  $T = 200$  K. In Fig. 1 we plot the electron densities in the spin-up and -down bands together with the incoherently summed spin coherence for  $N_i = 0$ . At  $t = 0$ , the initial spin polarization  $P = (N_{1/2} - N_{-1/2})/(N_{1/2} + N_{-1/2})$  is 2.5%. In this calculation, the Coulomb scattering is not included. It is seen from the figure that excess electrons in the spin-up band start to flip to the spin-down band at  $t = 0$  due to the presence of the magnetic field and the DP term  $\mathbf{h}(\mathbf{k})$ . In the meantime the spin coherence  $\rho$  accumulates. At about 9.7 ps, the electron densities in the two spin bands become equal and the spin coherence reaches its maximum. Then the spin coherence starts to feed back and the electron density in the spin-down band exceeds that in the spin-up band while  $\rho$  decreases. At about 18 ps,  $\rho$  reaches its minimum, while the density difference in the two spin bands reaches its maximum again with the excess electrons now in the spin-down band. Due to the dephasing, the second peak is lower than the first one. This oscillation goes on until the amplitude of the oscillation becomes zero due to the dephasing.

In Fig. 2, we plot the time evolution of electron densities in the two spin bands as well as the incoherently summed spin coherence for the same GaAs QW system as the previous one but taking the Coulomb scattering into account. The results without the Coulomb scatter-

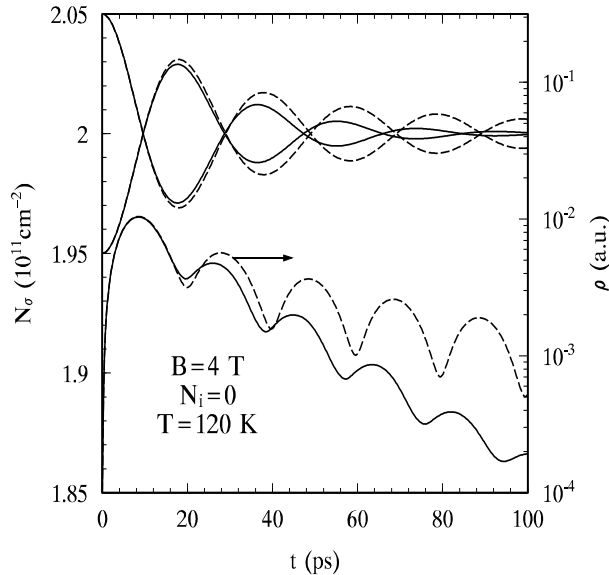


FIG. 2: Electron densities of up spin and down spin and the incoherently summed spin coherence  $\rho$  versus time  $t$  with (solid curves) and without (dashed curves) taking account the Coulomb scattering for a GaAs QW initial spin polarization  $P = 2.5\%$  at  $T = 120$  K. Note the scale of the spin coherence is on the right side of the figure.

ing are replotted as dashed curves in the figure. It is seen from the figure that for the first oscillation ( $t < 20$  ps), the electron densities as well as the spin coherences are almost the same in the presence and absence of the Coulomb scattering. As time goes on, the curves with the Coulomb scattering deviate from the ones without the Coulomb scattering. The decay rates of the excess spin density as well as the spin coherence are faster in the presence of Coulomb scattering.

It is known that, the Coulomb scattering is important only when the electron distribution is divagated from the Fermi function. In the first few picoseconds, the electrons in the two spin bands flip to their opposite bands due to the magnetic fields. The buildup of the inhomogeneity of  $\mathbf{k}$  in the electron distribution function comes from the DP term is marginal, and the electron distributions remain approximately the Fermi function. As time goes on, the effect of the DP term accumulates, the electron distribution functions divagate further and further away from the Fermi function and hence the Coulomb scattering becomes more and more important. Consequently, the spin signal that with the Coulomb scattering differs from the one without the Coulomb scattering. It has been pointed out that the spin dephasing due to the DP term and the SC scattering comes from two effects.<sup>24</sup> The first one is widely discussed that is due to the anisotropic property of the DP term, which, combined with SC scattering gives rise to the effective SF scattering.<sup>15,19</sup> In this case, inclusion of additional scattering enhances the momen-

tum relaxation rate and consequently reduces the spin dephasing rate.<sup>15,19,22</sup> It has been pointed out that the electron-electron Coulomb scattering, although does not contribute to the momentum relaxation rate, trends to reduce the spin dephasing<sup>38</sup> based on the similar analysis as in Refs. 15,19 and 22. The second is that the DP term itself also introduces an inhomogeneous broadening, which in the presence of the SC scattering provides *additional* spin dephasing channel<sup>22,24,25,26,27</sup> and therefore results in a faster spin dephasing. Our calculation self-consistently solves the Kinetic Bloch equations and includes *both* effects. The result indicates that for the present condition the second effect is more important and therefore the combined effect by inclusion of the Coulomb scattering leads to the increase of the spin dephasing.

### B. Spin polarization dependence of the spin dephasing time

We now turn to study the spin polarization dependence of the SDT. As our theory is a many-body theory and we include all the scattering, especially the Coulomb scattering, in our calculation, we are able to calculate the SDT with large spin polarization.

In Fig. 3, the SDT  $\tau$  is plotted against the initial spin polarization  $P$  for GaAs QW's with  $N_i = 0$  [Fig. 3(a)] and  $N_i = 0.1N_e$  [Fig. 3(b)] at different temperatures. The most striking feature of the impurity-free case is the huge increase of the SDT in low temperatures. For  $T = 120$  K, the SDT increases from 25 ps at low polarization to 720 ps at  $\sim 100\%$  polarization. In other words, the spin dephasing rate is decreased more than one order of magnitude when the spin polarization increases from 0 to 100 %. It is also seen from the figure that the increase of the SDT is reduced with the increase of temperature. For  $T = 300$  K, the SDT only gets an 80 % increase when the polarization increases from 0 to 100 %.

The dramatic increase in the  $\tau$ - $P$  curve in the low temperature regime originates from the electron-electron interaction, specifically the Hartree-Fock (HF) self-energy [*i.e.*, the last terms in the Eq. (4) and (6)]. As we know that the HF term itself does not contribute to the spin dephasing directly.<sup>22,27</sup> However, it behaves as an effective magnetic field which can alert the motion of the electron spins and can therefore affect the spin dephasing by combining with the DP term. For small spin polarization as commonly discussed in the literature, the contribution of the HF term is marginal. However, when the polarization gets higher, the HF contribution becomes larger. For example, the magnitude of the effective magnetic field of HF term is larger than 40 T, which is about ten folds of the applied magnetic field, for the case when the temperature is 120 K and the spin polarization is  $\sim 100\%$ . Differing from the applied magnetic field which in the Voigt configuration only gets the transverse components (*i.e.*  $B_x$  and  $B_y$ ) and always causes the electrons to flip between spin-up and -down bands, the effective magnetic

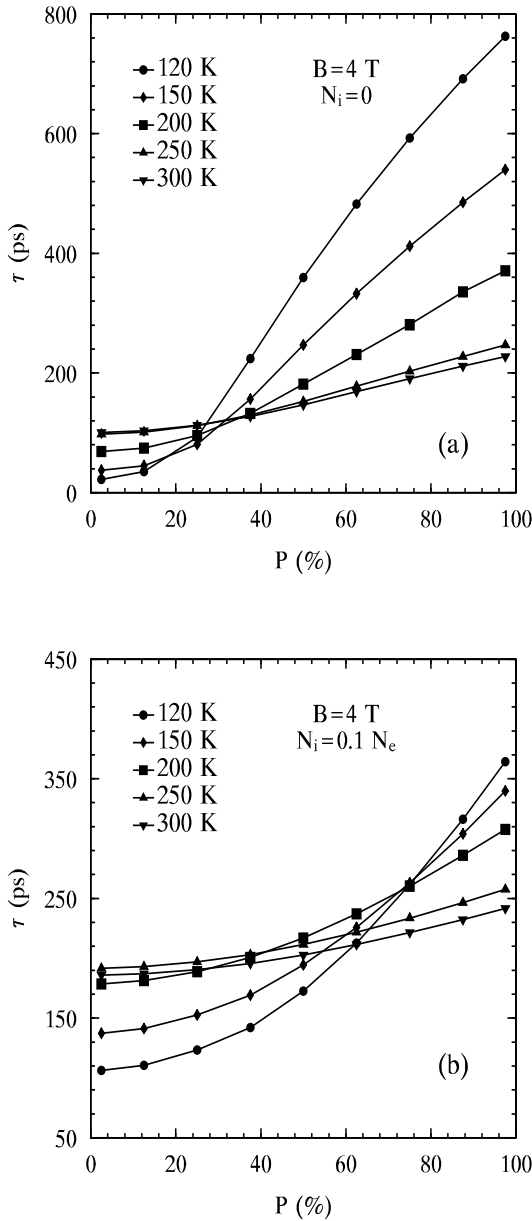


FIG. 3: Spin dephasing time  $\tau$  versus the initial spin polarization with different impurity concentration and different temperatures. The impurity densities in (a) and (b) are 0 and  $0.1N_e$  respectively. The lines are plotted for the aid of eyes.

field formed by the HF term contains a longitudinal component [ $B_z^{\text{HF}}(\mathbf{k})$ ] which can effectively reduce the “detuning” of the spin-up and -down electrons, and thus strongly reduces the spin dephasing. In order to show this detuning effect, we remove the longitudinal component of the effective magnetic field  $B_z^{\text{HF}}(\mathbf{k})$  and recalculate the SDT at the temperature of 120 K for different initial spin polarization for an impurity free sample. The result is plotted in Fig. 4. From the figure one can see

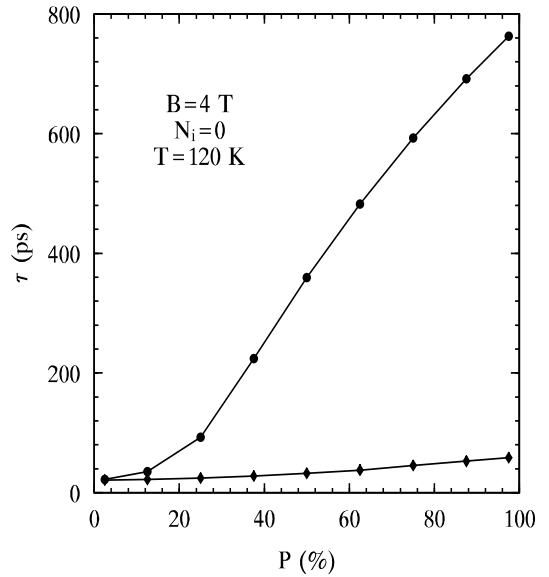


FIG. 4: Spin dephasing time  $\tau$  versus the initial spin polarization  $P$  for at  $T = 120$  K and  $N_i = 0$ . Circle (●): With the longitudinal component of HF term included; Diamond (◆): Without the longitudinal component of HF term include. The lines are plotted for the aid of eyes.

that when the longitudinal component of the HF term is removed, the dramatic increase in the  $\tau$ - $P$  curve disappears and the SDT is insensitive to the initial spin polarization.

When the temperature increases, for a given initial spin polarization the HF term becomes smaller as the electrons are distributed to a wider range in the  $\mathbf{k}$ -space. Therefore the effect of the HF term becomes smaller too. Consequently the increase in the  $\tau$ - $P$  curve becomes slower.

The  $\tau$ - $P$  curve gets flatter when the impurities are introduced. It is shown from Fig. 3(b) that, when the density of impurity is large, say  $N_i = 0.1N_e$ , the fast rise in the  $\tau$ - $P$  curve in low temperature regime still remains. Nevertheless the rate of increase is much smaller than the corresponding one when the impurities are absent.

To further reveal the contribution of the impurity to the dephasing under different conditions, we plot the SDT as a function of the polarization for different impurity levels at  $T = 120$  K in Fig. 5. The figure clearly shows that when the impurity concentration increases, the slope of the  $\tau$ - $P$  curve becomes smaller. This is because that impurity scattering reduces the HF term and the effect of the longitudinal component of the HF term is also reduced. Consequently, the increase of SDT with the polarization is reduced.

It is interesting to note that contrary to the high polarization regime where the SDT decreases with the impurity concentration, the spin dephasing is reduced by the impurity scattering in the low polarization regime. As

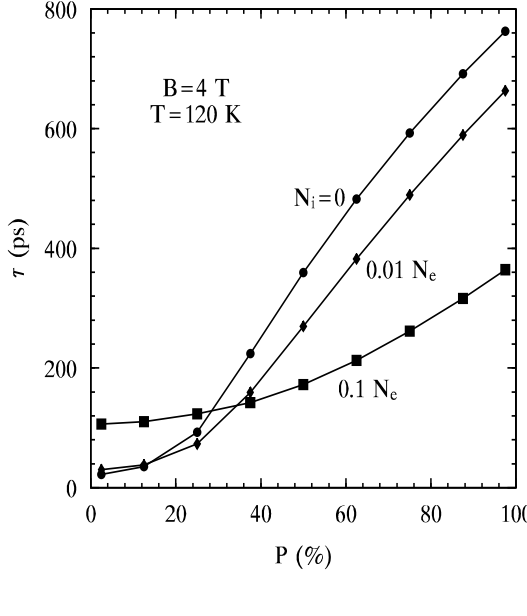


FIG. 5: Spin dephasing time  $\tau$  versus the initial spin polarization  $P$  at  $T = 120$  K for different impurity levels. Circle (●):  $N_i = 0$ ; Diamond (◆):  $N_i = 0.01N_e$ ; Square (■):  $N_i = 0.1N_e$ . The lines are plotted for the aid of eyes.

we pointed out before that the impurities affect the spin dephasing in two ways.<sup>24</sup> On the one hand, the electron-impurity scattering provides a new spin dephasing channel by combining with the DP term<sup>19,24</sup> to give an effective SF scattering through the inhomogeneous broadening introduced by the DP term. This gives rise to the enhancement of the dephasing. On the other hand, the scattering also redistributes the electrons in the momentum space and leads them to an isotropic distribution. Therefore, the scattering can suppress the anisotropy caused by the DP term, consequently the effective SF scattering. Moreover, the suppression of the anisotropy also corresponds to the reduction of the inhomogeneous broadening. Both lead to a smaller spin dephasing. Our results indicate that in the low temperature and the low polarization regime, the impurities tend to reduce the spin dephasing.

### C. The temperature dependence of the spin dephasing time

Above we discussed the dependence of spin dephasing on initial spin polarization for different temperatures. Now we turn to the temperature dependence of the SDT under different initial spin polarizations. From Fig. 3(a) and (b) in Sec. III(B), one can see that for small spin polarization, the SDT increases with the temperature. Whereas in high polarized regime, the SDT decreases with the temperature. For moderate polarization, the

temperature dependence is too complicated to be described by a monotonic function of temperature. Under certain condition, the SDT can be insensitive to the temperature, e.g. the SDT is almost unchanged with the temperature when the polarization  $P = 75\%$  and  $N_i = 0.1N_e$ .

To see more detail of how the spin dephasing depends on the temperature, we replot in Fig. 6(a) and (b) the SDT shown in Figs. 3 and 4 as a function of the temperature for different impurity levels and different spin polarizations. It is seen from the figure that, for low polarization, the SDT increases systematically with the temperature for all impurity levels. This property is *opposite* to the results of earlier simplified treatments of the DP effect, where it was predicted that the spin lifetime decreases with the increase of temperature in the 2D system.<sup>39,40</sup> The SDT based on the simplified model is given by<sup>26,39,41</sup>

$$\frac{1}{\tau} = \frac{\int_0^\infty dE_k (f_{k\frac{1}{2}} - f_{k-\frac{1}{2}}) \Gamma(k)}{\int_0^\infty dE_k (f_{k\frac{1}{2}} - f_{k-\frac{1}{2}})}, \quad (10)$$

in which

$$\begin{aligned} \Gamma(k) = & 2\tau_1(k) \left[ (\gamma \langle k_z^2 \rangle)^2 k^2 - \frac{1}{2} \gamma \langle k_z^2 \rangle k^4 \right. \\ & \left. + \frac{1 + \tau_3(k)/\tau_1(k)}{16} \gamma^2 k^6 \right] \end{aligned} \quad (11)$$

and

$$\tau_n^{-1}(k) = \int_0^{2\pi} \sigma(E_k, \theta) [1 - \cos(n\theta)] d\theta. \quad (12)$$

$\sigma(E_k, \theta)$  stands for scattering cross-section. For comparison, we plot the SDT predicated by the earlier model and by our present many-body theory in the inset of Fig. 6(a). From the inset one can see that the SDT predicated by the earlier model is about one order of magnitude larger than the one predicated by our theory. In the mean time, the SDT of the earlier mode drops dramatically with the increase of the temperature. Nevertheless, in our many-body treatment, it rises slightly with the temperature.

The recent experiments show that the SDT in  $n$ -type quantum wells increases slightly with the increase of temperature,<sup>42</sup> or is almost unchanged with the temperature.<sup>43</sup> It is also noted that the SDT's measured in the experiment<sup>43</sup> for GaAs QW are with the regime of values predicted by our theory, but one order of magnitude smaller than those by the earlier model. Moreover, it has been reported very recently that there is a big discrepancy between the earlier simplified treatment of the DP effect and the experiment on the SDT. It is shown that the theoretical SDT is about one order of magnitude larger than the experiment data in  $n$ -type bulk GaAs for certain electron densities.<sup>44</sup>

It is seen that our many-body result is better than the earlier simplified treatments both qualitatively and quantitatively. The reason that our model is more precise than the earlier one lies on the fact that the earlier

model is based on the single particle picture which does not count for the dephasing due to the inhomogeneous broadening inherited in the DP term, which is the result of the many body effect.<sup>22,24,25,26,27</sup> By comparing the theoretical SDT predicated by the two models, we can see that the spin dephasing due to the inhomogeneous broadening is much more important. In the case we calculated, the spin dephasing is dominated by the inhomogeneous broadening. Therefore, it is easy to understand why the earlier simplified treatment of the DP mechanism gives much slower spin dephasing.

The temperature dependence of the SDT can be understood once the spin dephasing due to the inhomogeneous broadening is taken into account: When the temperature increases, the inhomogeneous broadening is reduced as the electrons are distributed to the wider  $k$ -states. As a result, the number of electron occupation on each  $\mathbf{k}$  state is reduced. It is further noted that this reduction is mild as a function of the temperature. Therefore, the temperature dependence is quite mild unless it is within the regime where the HF term plays an important role in the spin dephasing.

In the region where the HF term is important, in addition to the above mentioned two effects of the temperature on the spin dephasing, the temperature dependence of the HF term should also be taken into account. In general, the temperature dependence of the SDT due to the combination of these three effects is too complicated to be described by a monotonic function. We replot the SDT as a function of the temperature in Fig. 6(b), for a typical high polarization  $P = 75\%$ . We can see that due to the reduction of the HF term, the reduction of the detuning is removed and SDT drops dramatically with the increase of the temperature in the impurities free sample. While for the system with impurity concentration  $N_i = 0.1N_e$ , the HF term is not as important as in the impurities free sample, and the SDT is insensitive to the temperature.

#### D. Magnetic field dependence of the spin dephasing

We now investigate the magnetic field dependence of the spin dephasing. In Fig. 7, we plot the SDT versus the applied magnetic field for different impurity levels and different spin polarizations. It is seen from the figure that in small polarization regime for both impurity free and doped samples, the SDT is almost a constant when the magnetic field varies from 1 T to 8 T. Whereas, in the high polarization regime, the SDT increases with the magnetic field when the magnetic field varies from 1 T to 4 T and then saturates when the magnetic field is larger than 4 T. It is noted that the transverse magnetic field imposes two effects on the spin dephasing. One is that in the presence of a magnetic field, the electron spins undergo a Larmor precession around the magnetic field. This precession suppresses the precession about the

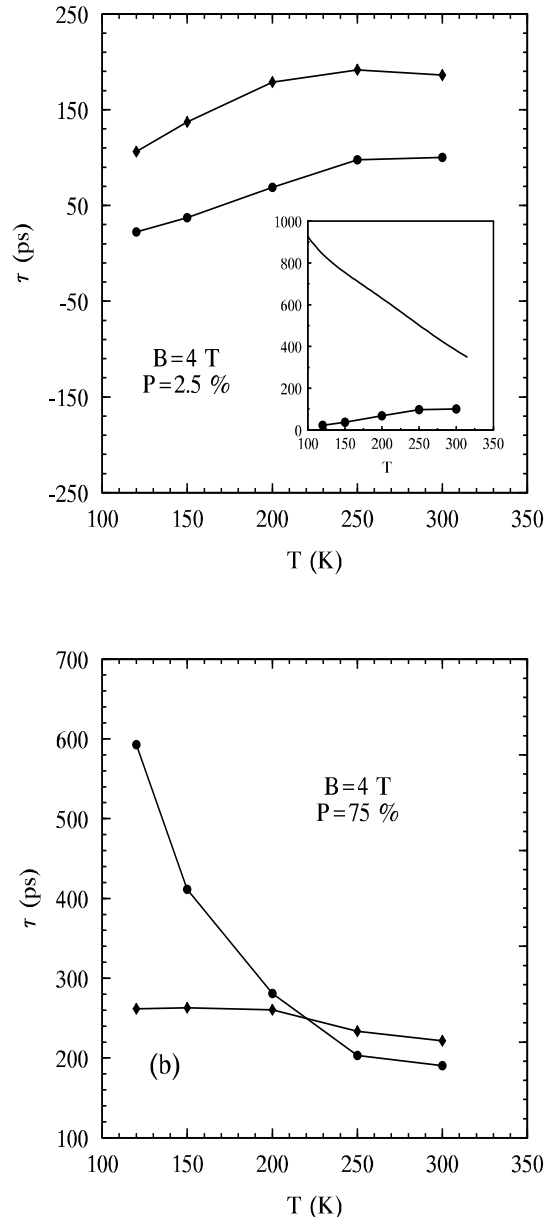


FIG. 6: Spin dephasing time  $\tau$  versus the temperature  $T$  with spin polarization  $P = 2.5\%$  (a) and  $P = 75\%$  (b) under two different impurity levels. Circle (●):  $N_i = 0$ ; Square (■):  $N_i = 0.1N_e$ . The lines are plotted for eye aid. The SDT predicated by the simplified treatment of DP term (solid curve) and our model (circle) for  $N_i = 0$  is plotted in the inset of (a) for comparison.

effective magnetic field  $\mathbf{h}(\mathbf{k})$  of the DP term.<sup>15,45</sup> Therefore the SDT increases with the magnetic field. However, in the presence of the transverse magnetic field, the spin precession frequency between the spin-up and -down band is  $\sqrt{(g\mu_B B - h_x(\mathbf{k}))^2 + h_y^2(\mathbf{k})}$ . Hence the transverse magnetic field may introduce an additional

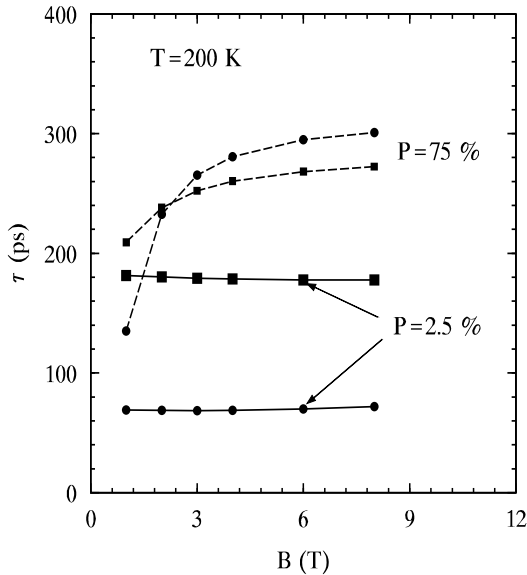


FIG. 7: Spin dephasing time  $\tau$  versus the applied magnetic field for different spin polarizations and different impurity levels. Solid curve with dots:  $N_i = 0$ ,  $P = 2.5\%$ ; Solid curve with squares:  $N_i = 0.1N_e$ ,  $P = 2.5\%$ ; Dashed curve with dots:  $N_i = 0$ ,  $P = 75\%$ ; Dashed curve with squares:  $N_i = 0.1N_e$ ,  $P = 75\%$ .

inhomogeneous broadening for the electrons and consequently results in a shorter SDT. In the cases we study, the SDT is almost unchanged with the magnetic field with the combined contributions from these two effects.

In addition to the above mentioned effects of the magnetic field on the spin dephasing, one can further see from Fig. 7, that for large spin polarization, the magnetic field enhances the SDT. As we mentioned before, for large spin polarization, the contribution from the HF term is important. Therefore, the magnetic field can further affect the spin dephasing rate through the enhancement of the HF term in the high initial spin polarization regime. It is shown in the figure that, for high initial spin polarization, when the magnetic field increases, the enhanced HF term results in a fast decrease of spin dephasing rate. Nevertheless, after the magnetic field is high enough, the HF term arrives at maximum. As a result, the SDT saturates with the magnetic field.

### E. Electron density dependence of spin dephasing

We now turn to the electron density dependence of the spin dephasing. In Fig. 8 we plot the SDT as a function of the electron density for both low and high spin polarizations. It can be seen from the figure that for low polarization, the SDT decreases with electron density: from 70 ps for  $N_e = 4 \times 10^{11} \text{ cm}^{-2}$  to 4 ps for  $N_e = 40 \times 10^{11} \text{ cm}^{-2}$ . This is because with the increase

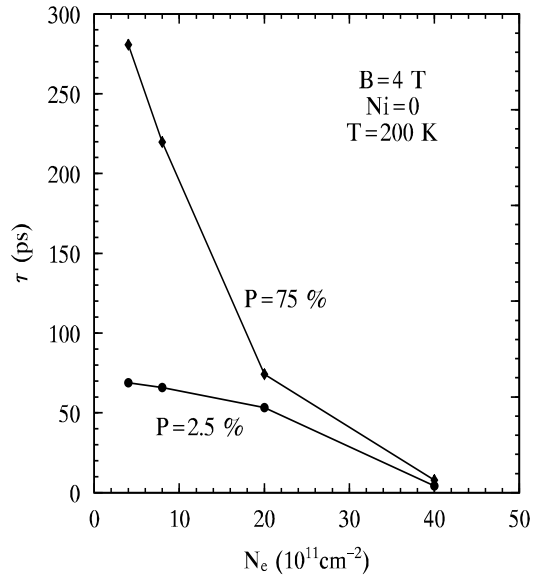


FIG. 8: Spin dephasing time  $\tau$  versus the total electron density  $N_e$  for a GaAs QW with  $T = 200 \text{ K}$ ,  $B = 4 \text{ T}$ ,  $N_i = 0$  and  $P = 2.5\%$  (●) and  $P = 75\%$  (◆). The lines are plotted for the aid of eyes.

of the electron density, more electrons are distributed at large momentum states and strengthen the DP effect as the DP term increases with the momentum. For the high spin polarization, the SDT also decreases with the electron density, however, with a much faster speed. When the initial spin polarization is 75%, the SDT decreases from 280 ps for  $N_e = 4 \times 10^{11} \text{ cm}^{-2}$  to 8 ps for  $N_e = 40 \times 10^{11} \text{ cm}^{-2}$ . This is understood that when the electron density increases, the effect of HF term becomes less important comparing to the increase of the DP term.

### F. The effect of quantum well width on the spin dephasing

It is noted from the experiments that the SDT of quantum wells is much smaller than that of bulk material. This is because the DP term in the quasi-two dimensional quantum well contains a term which is proportional to the  $\langle k_z^2 \rangle = (\pi/a)^2$ . For a regular quantum well in the order of 10 nm, this term is much larger than the square of Fermi vector  $k_F^2$ , when the electron density is up to the order of  $10^{11} \text{ cm}^{-2}$ . Therefore the DP term in the quantum well is greatly enhanced. Moreover, the smaller the width is, the larger the DP term becomes and the faster the SDT turns to be. In this subsection we study the effect of the quantum well width on the spin dephasing. In Fig. 9 the SDT is plotted as a function of the initial spin polarization for three different widths. Moreover, in Figs. 10(a) and (b) we plot the SDT as a function

of the temperature for two initial spin polarizations in three different quantum wells. These figures clearly show that, for all situations, the spin dephasing rate decreases with the increase of the well width. Especially when the width is decreased by only 50 % from 20 nm, the SDT is reduced by one order of magnitude.

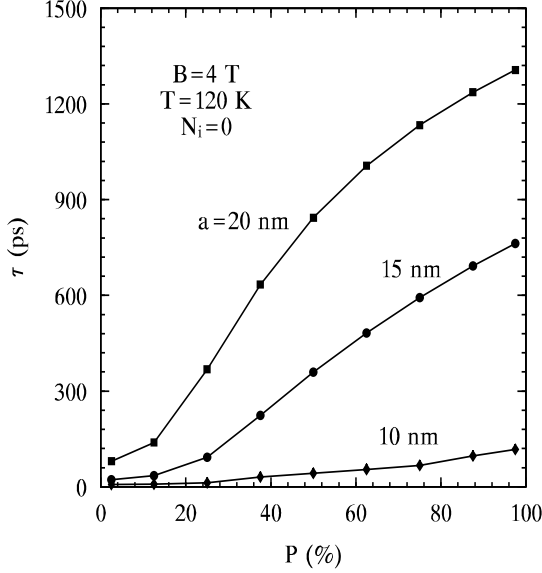


FIG. 9: Spin dephasing time  $\tau$  versus the initial spin polarization  $P$  at  $T = 120$  K and  $N_i = 0$  in three quantum wells with different widths: Diamond ( $\blacklozenge$ ):  $a = 10$  nm; Circle ( $\bullet$ ):  $a = 15$  nm; Square ( $\blacksquare$ ):  $a = 20$  nm. The lines are plotted for the aid of eyes.

#### IV. CONCLUSION

In conclusion, we have performed a systematic investigation of the DP effect on the spin dephasing of  $n$ -typed GaAs QW's for high temperatures under moderate magnetic fields in Voigt configuration. Based on the nonequilibrium Green's function theory, we derived a set of kinetic Bloch equations for a two-spin-band model. This model includes the electron-phonon, electron-impurity scattering as well as the electron-electron interaction. By numerically solving the kinetic Bloch equations, we study the time evolution of electron densities in each spin band and the spin coherence – the correlation between spin-up and -down bands. The spin dephasing time is calculated from the slope of the envelope of the time evolution of the incoherently summed spin coherence. We therefore are able to study in detail how this dephasing time is affected by spin polarization, temperature, impurity level, magnetic field and electron density. Different from the earlier studies on spin dephasing based on the single particle model which only considers the effective SF scatter-

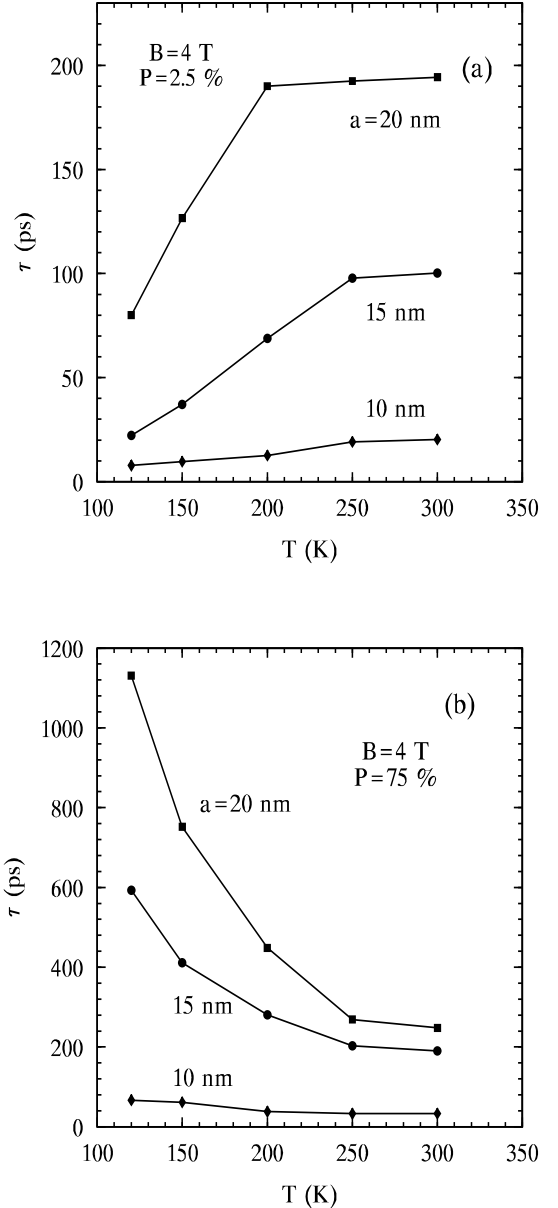


FIG. 10: Spin dephasing time  $\tau$  versus temperature  $T$  in three quantum wells with different widths: Diamond ( $\blacklozenge$ ):  $a = 10$  nm; Circle ( $\bullet$ ):  $a = 15$  nm; Square ( $\blacksquare$ ):  $a = 20$  nm. (a), the initial spin polarization  $P = 2.5$  %; (b)  $P = 75$  %. The lines are plotted for the aid of eyes.

ing, our theory also takes account of the contribution of many-body effect on the spin dephasing.<sup>22,24,25,26,27</sup> In fact, for the  $n$ -typed semiconductors and the spin polarization studied in the experiments, this many-body dephasing effect is even more important than the effective SF scattering as it can be one order of magnitude larger than the later. Equally remarkable is that, as we include all the scattering, especially the Coulomb scattering in

our many-body theory, now we are able to calculate the spin dephasing with extra large (up to 100 %) initial spin polarization.

It is discovered that the SDT increases dramatically with the initial spin polarization. We stress here that the SDT is defined to be the inverse of the spin dephasing rate, instead of the total life time which naturally increases with the initial spin polarization. At low impurity level and for low temperature, the magnitude of SDT increases more than one order when the initial polarization goes from 0 to 100 %. It is discovered that this dramatic increase originates from the HF contribution of the electron-electron Coulomb interaction. The HF term forms an effective magnetic field which affects the spin dephasing. As the longitudinal component of the HF term effectively reduces the “detuning” between the spin-up and -down bands, the spin dephasing becomes much slower in high polarization region. Due to the fact that the dramatic increase comes from the HF term, the magnitude of the increase is therefore affected by all the factors that influences the HF term, such as temperature, impurity scattering, magnetic field as well as the electron density. When the temperature or the impurity density increases, the effective magnetic field formed by the HF term for a given initial spin polarization decreases. Therefore, the increase in  $\tau$ - $P$  curve is reduced, and the  $\tau$ - $P$  curve becomes flatter. Nevertheless when the magnetic field increases, the HF term is enhanced and the increase in the  $\tau$ - $P$  is enhanced accordingly. When the magnetic field increases beyond 4 T, the HF saturates. Consequently after 4 T, the increase in  $\tau$ - $P$  curves only gets slight changes with the magnetic field.

For low spin polarized regime, the SDT increases with the temperature. This is contrary to the result of earlier simplified single-particle calculation where the SDT always decreases with the increase of the temperature. Moreover, the SDT predicted by our many-body calculation is one order of magnitude faster than the earlier result. We show that our results are in agreement with the experiments both qualitatively and quantitatively. The physics of this feature is due to the additional many-body spin dephasing channel due to the inhomogeneous broadening provided by the DP term, which by combining with the SC scattering also causes spin dephasing. In the situation we studied, the spin dephasing is dominated by the many-body dephasing effect. With the increase of the temperature, the inhomogeneous broadening reduces and the SDT increases.

The effect of the electron-impurity scattering on the spin dephasing is also studied. The SDT increases in the presence of the impurity scattering. This is because

the impurity scattering redistributes the electrons to an isotropic state which in turn reduces the spin dephasing.

In high spin polarization region, in addition to the above mentioned role the scattering plays in the spin dephasing, the scattering also affects the HF term. This brings more complication in the study of the spin dephasing. In general the SDT can not be described by a monotonic function of the temperature or the impurity concentration in high polarization region. For a typically high initial spin polarization,  $P = 75 \%$ , the SDT decreases dramatically with the temperature as the reduction of the detuning is suppressed when the temperature increases. Whereas when the impurity concentration is  $0.1N_e$ , the SDT is insensitive to the temperature.

As the magnetic field causes the electron spins to precess about it, this precession will suppress the precession about the effective magnetic field  $\mathbf{h}(\mathbf{k})$  originated from the DP effect. However, the transverse magnetic field in the Voigt configuration also introduces additional inhomogeneous broadening in the momentum space and enhances the spin dephasing. As a result of the combining effects, for the condition we studied, the spin dephasing is almost unchanged with the magnetic field in low spin polarization region. The magnetic field also enhances the HF term, therefore the  $\tau$ - $B$  curve gets a faster increase in the high polarization region when the magnetic field is smaller than 4 T. In the region of the magnetic field higher than 4 T, the HF term achieves its maximum. The effect of the magnetic field on the HF term saturates, the SDT saturates accordingly.

Our calculation also shows that when the electron density increases, the SDT decreases. This is because with the increase of the electron density, more electrons are distributed at larger momentum states and consequently the DP term is strengthened. While as the width of the quantum well increases, the SDT decreases as the DP term reduces.

In summary we have performed a thorough investigation of the spin dephasing in  $n$ -typed GaAs QW's for high temperatures. Many new features which have not been investigated both theoretically and experimentally are predicted in a wide range of parameters.

## Acknowledgments

MWW is supported by the “100 Person Project” of Chinese Academy of Sciences and Natural Science Foundation of China under Grant No. 10247002.

---

\* Author to whom correspondence should be addressed;  
Electronic address: mwwu@ustc.edu.cn

† Mailing Address.

<sup>1</sup> T. C. Damen, L. Vina, J. E. Cunningham, J. Shah, and L. J. Sham, Phys. Rev. Lett. **67**, 3432 (1991).

<sup>2</sup> J. Wagner, H. Schneider, D. Richards, A. Fischer, and

K. Ploog, Phys. Rev. B **47**, 4786 (1993).

<sup>3</sup> J. J. Baumberg, S. A. Crooker, D. D. Awschalom, N. Samarth, H. Luo, and J. K. Furdyna, Phys. Rev. Lett. **72**, 717 (1994).

<sup>4</sup> J. J. Baumberg, S. A. Crooker, D. D. Awschalom, N. Samarth, H. Luo, and J. K. Furdyna, Phys. Rev. B **50**, 7689 (1994).

<sup>5</sup> A. P. Heberle, W. W. Rühle, and K. Ploog, Phys. Rev. Lett. **72**, 3887 (1994).

<sup>6</sup> C. Buss, R. Frey, C. Flytzanis, and J. Cibert, Solid State Commun. **94**, 543 (1995).

<sup>7</sup> S. A. Crooker, J. J. Baumberg, F. Flack, N. Samarth, and D. D. Awschalom, Phys. Rev. Lett. **77**, 2814 (1996).

<sup>8</sup> S. A. Crooker, D. D. Awschalom, J. J. Baumberg, F. Flack, and N. Samarth, Phys. Rev. B **56**, 7574 (1996).

<sup>9</sup> C. Buss, R. Pankoke, P. Leisching, J. Cibert, R. Frey, and C. Flytzanis, Phys. Rev. Lett. **78**, 4123 (1997).

<sup>10</sup> J. M. Kikkawa, I. P. Smorchkova, N. Samarth, and D. D. Awschalom, Science **277**, 1284 (1997).

<sup>11</sup> J. M. Kikkawa and D. D. Awschalom, Nature **397**, 139 (1998).

<sup>12</sup> J. Kikkawa and D. Awschalom, Phys. Rev. Lett. **80**, 4313 (1998).

<sup>13</sup> H. Ohno, Science **281**, 951 (1998).

<sup>14</sup> Y. Ohno, R. Terauchi, T. Adachi, F. Matsukura, and H. Ohno, Phys. Rev. Lett. **83**, 4196 (1999).

<sup>15</sup> F. Meier and B. P. Z. (Eds), *Optical Orientation* (North-Holland, Amsterdam, 1984).

<sup>16</sup> A. G. Aronov, G. E. Pikus, and A. N. Titkov, Zh. Eksp. Teor. Fiz. **84**, 1170 (1983), [Sov. Phys.-JETP **57**, 680 (1983)].

<sup>17</sup> Y. Yafet, Phys. Rev. **85**, 478 (1952).

<sup>18</sup> R. J. Elliot, Phys. Rev. **96**, 266 (1954).

<sup>19</sup> M. I. D'yakonov and V. I. Perel', Zh. Eksp. Teor. Fiz. **60**, 1954 (1971), [Sov. Phys.-JETP **38**, 1053 (1971)].

<sup>20</sup> G. L. Bir, A. G. Aronov, and G. E. Pikus, Zh. Eksp. Teor. Fiz. **69**, 1382 (1975), [Sov. Phys.-JETP **42**, 705 (1975)].

<sup>21</sup> Haug and A. P. Jauho, *Quantum Kinetics in Transport and Optics of Semiconductors* (Springer-Verlag, Berlin, 1996).

<sup>22</sup> M. W. Wu, J. Supercond.: Incorporating Novel Mechanism **14**, 245 (2001), cond-mat/0109258.

<sup>23</sup> M. W. Wu and H. Metiu, Phys. Rev. B **61**, 2945 (2000).

<sup>24</sup> M. W. Wu and C. Z. Ning, phys. stat. sol. B **222**, 523 (2000).

<sup>25</sup> M. W. Wu and M. Kuwata-Gonokami, Solid State Commun. **121**, 509 (2002).

<sup>26</sup> M. W. Wu, J. Phys. Soc. Jap. **70**, 2195 (2001).

<sup>27</sup> M. W. Wu and C. Z. Ning, Eur. Phys. J. B. **18**, 373 (2000).

<sup>28</sup> M. Q. Weng and M. W. Wu, Phys. Rev. B **66**, 235109 (2002).

<sup>29</sup> M. Q. Weng and M. W. Wu, J. Appl. Phys. **93**, 410 (2003).

<sup>30</sup> G. Dresselhaus, Phys. Rev. **100**, 580 (1955).

<sup>31</sup> Y. A. Bychkov and E. Rashba, J. Phys. C **17**, 6039 (1984).

<sup>32</sup> Y. A. Bychkov and E. Rashba, Sov. Phys. JETP Lett. **39**, 78 (1984).

<sup>33</sup> R. Eppenga and M. F. H. Schuurmans, Phys. Rev. B **37**, 10923 (1988).

<sup>34</sup> E. L. Ivchenko and G. E. Pikus, *Superlattices and Other Heterostructures* (Springer, Berlin, 1995).

<sup>35</sup> G. D. Mahan, *Many-particle Physics* (Plenum, New York, 1981).

<sup>36</sup> T. Kuhn and F. Rossi, Phys. Rev. Lett. **69**, 977 (1992).

<sup>37</sup> O. Madelung, M. Schultz, and H. W. (eds.), *Numerical Data and Functional Relationships in Science and Technology, Landolt-Börnstein, New Series*, vol. 17 (Springer-Verlag, Berlin, 1982).

<sup>38</sup> M. M. Glazov and E. L. Ivchenko, Pis'ma Zh. Eksp. Teor. Fiz. **75**, 476 (2002), [JETP Lett. **75**, 403 (2002)].

<sup>39</sup> N. S. Averkiev, L. E. Golub, and M. Willander, J. Phys.: Cond. Mat. **14**, R271 (2002).

<sup>40</sup> M. I. Dyakonov and V. Y. Kachorovskii, Fiz. Tekh. Poluprovodn. **20**, 178 (1986), [Soviet Phys. - Semicond. **20**, 110 (1986)].

<sup>41</sup> W. H. Lau, J. T. Oleberg, and M. E. Flatté, Phys. Rev. B **64**, 161301 (2001).

<sup>42</sup> D. Hägele, M. Oestreich, W. Rühle, J. Hoffmann, S. Wachter, H. Kalt, K. Ohkawa, and D. Hommel, Physica B **272**, 338 (1999).

<sup>43</sup> A. Malinowski, R. S. Britton, T. Grevatt, R. T. Harley, D. A. Ritchie, and M. Y. Simmons, Phys. Rev. B **62**, 13034 (2000).

<sup>44</sup> P. H. Song and K. W. Kim, Phys. Rev. B **66**, 035207 (2002).

<sup>45</sup> F. X. Bronold, I. Martin, A. Saxena, and D. L. Smith (2002), cond-mat/0208139.